Entanglement swapping between dissipative systems

A. Nourmandipour[1,*] and M. K. Tavassoly[1,2,†]
[1]*Atomic and Molecular Group, Faculty of Physics, Yazd University, 89195-741 Yazd, Iran*
[2]*Photonic Research Group, Engineering Research Center, Yazd University, 89195-741 Yazd, Iran*
(Received 21 June 2016; published 29 August 2016)

In this paper, we investigate the possibility of entanglement swapping between two distinct qubits coupled to their own (in general) non-Markovian environments. This goal is achieved by performing Bell state measurement on photons leaving dissipative cavities. In the continuation, we introduce the concept of entangling power to measure the average of swapped entanglement over all possible pure initial states. Then we present our results in two regimes, strong and weak coupling, and discuss the role of the detuning parameter in each regime in the amount of swapped entanglement. We also determine the conditions under which the maximum amount of entanglement can be swapped between the two qubits. It is revealed that, despite the presence of dissipation, it is possible to create long-living stationary entanglement between the two qubits.

DOI: 10.1103/PhysRevA.94.022339

I. INTRODUCTION

Recently, a great deal of attention has been devoted to the concept of quantum entanglement [1] due to its various applications such as quantum cryptography [2], quantum teleportation [3], superdense coding [4], sensitive measurements [5], and quantum telecloning [6]. There are many implementations to produce entangled states like trapped ions [7], atomic ensembles [8], photon pairs [9], and superconducting qubits [10]. However, it is well known that the interaction of atoms with various types of cavity fields (with additional interaction terms such as Kerr medium, etc.) is an efficient source of entanglement [11], a model which is called the Jaynes-Cummings model (JCM) [12]. It relies on the mutual coupling between a two-level atom and a single-mode quantized field in the rotating-wave approximation.

On the other hand, this idea has been put forward that it is possible to create entanglement between subsystems distributed over long distances without any common past. In such cases, one could think of entangling the subsystems by constructing a more general system, with the help of two (or more) other entangled quantum subsystems, a phenomenon which is called quantum swapping [13]. This notion was originally proposed for swapping the entanglement between a pair of particles [13] and later was generalized to multiparticle quantum systems [14]. It has also been shown that it is possible to implement quantum swapping for continuous variable systems [15]. Experimental demonstration of unconditional entanglement swapping for continuous variables has been investigated in [16]. The possibility of optimization of entanglement purification via entanglement swapping has been studied in [17]. Entanglement swapping in two independent JCMs has been discussed in [18]. In particular, very recently the influence of Kerr medium on the entanglement swapping in a three-level atom-atom system has been considered by one of us [19].

In addition, by replacing the unknown state with an entangled state, entanglement swapping can be considered a special example of quantum teleportation [20,21]. The basic concept concealed behind quantum swapping is the Bell state measurement (BSM) approach. This notion can be thought of as a projection operator which projects the state of fields into a Bell state and leaves qubits in an entangled state [22].

However, dissipation is ever present in real physical systems. This is due to the unavoidable interaction between these systems and their surrounding environments, which usually leads to loss of entanglement stored in the systems. Therefore, a lot of attention has been paid on the theory of open quantum systems [23,24]. In this regard, besides considering the Lindblad master equation, which is based on the temporal evolution of the density operator of the system [24], one can deal with the time evolution of the wave function of the system instead of the density operator by solving the time-dependent Schrödinger equation. Recently, this approach has been used by us to investigate the dynamics of entanglement of two qubits in separate environments [25] and of two [26] and an arbitrary number [27,28] of qubits in a common environment. Altogether, it seems quite logical to investigate different aspects of quantum information processing, especially quantum entanglement swapping, in the presence of dissipation.

In this paper, we study the possibility of entanglement swapping between two independent subsystems in the presence of dissipation. To this end, we consider each subsystem as a dissipative cavity, in each of which there is a two-level atom interacting with a cavity field, and the cavity mode itself interacts with the surrounding environment. We model the surrounding environment as a set of continuous harmonic oscillators. This allows us to obtain the exact time evolution of the wave function of each atom-environment subsystem as a function of the environment correlation time and investigate the dynamics of entanglement of each subsystem outside the Markovian regime for both weak- and strong-coupling regimes by paying attention to the linear entropy. Then, with the help of BSM performed on the fields leaving the cavities, we show that how the produced atom-field entanglement can be swapped between field-feld and atom-atom results in a final (possible) atom-atom entangled state in the presence of dissipation. Next, we quantify the amount of entanglement via concurrence [29]. We then use an entangling power measure by generalizing

*anoormandip@stu.yazd.ac.ir
†mktavassoly@yazd.ac.ir

the expression used for unitary maps [30] in order to see, on average, how much entanglement can be swapped between two atoms. The entangling power relies on the statistical average over the initial states, which establishes an input-independent dynamics of entanglement: a concept that has already been applied in many quantum systems [31,32].

The rest of the paper is organized as follows: In Sec. II, we introduce our modeling of dissipation of the system under consideration and obtain the explicit form of the state vector of the entire system at any time t. In Sec. III we investigate the dynamics of the linear entropy of each subsystem. Section IV deals with the dynamical behavior of the entangling power of the atom-atom state after BSM for two types of Bell states of cavities fields. Finally, in Sec. V we draw our conclusions.

II. MODEL

The system under consideration consists of two similar but separate dissipative cavities, each containing a two-level atom with an excited (ground) state $|e\rangle$ ($|g\rangle$). We model each dissipative cavity as a high-Q cavity in which the qubit interacts with a single-mode field, however, the field itself interacts with an external field which is considered as a set of continuous harmonic oscillators (see Fig. 1). The correlation between the qubit and the field in each cavity via the coupling constant g_i is characterized by terms like $g_i(\hat{\sigma}_i^+\hat{a}_i + \hat{\sigma}_i^-\hat{a}_i^\dagger)$, in which $\hat{\sigma}_i^+$ ($\hat{\sigma}_i^-$) is the raising (lowering) operator of the ith qubit and $\hat{a}_i$ ($\hat{a}_i^\dagger$) is the annihilation (creation) operator of the ith cavity field. The interaction between the cavity and the external field in the ith cavity can be governed by the Hamiltonian

$$\hat{H}_{\mathrm{I}_i} = \omega_{c_i}\hat{a}_i^\dagger\hat{a}_i + \int_0^\infty \eta\hat{B}_i^\dagger(\eta)\hat{B}_i(\eta)\,d\eta + \int_0^\infty [G_i(\eta)\hat{a}_i^\dagger\hat{B}_i(\eta) + \mathrm{H.c.}]\,d\eta, \quad (1)$$

where ω_{c_i} is the frequency of the ith cavity field, $G_i(\eta)$ is the coupling coefficient, which, in general, is a function of the frequency that connects the external world to the ith cavity, and $\hat{B}_i^\dagger(\eta)$ and $\hat{B}_i(\eta)$ are the creation and annihilation operators of the ith surrounding environment in mode η, which

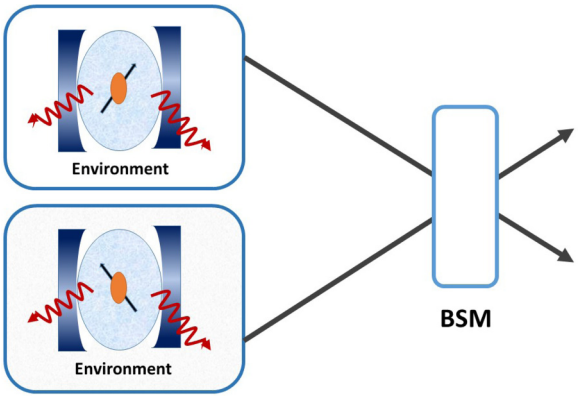

FIG. 1. Pictorial representation of the entanglement swapping. Each qubit has been placed in its own cavity in the presence of dissipation. BSM is performed on photons leaving the environments, which leads to the establishment of entanglement between the atoms.

obey the commutation relation $[\hat{B}_i(\eta), \hat{B}_j^\dagger(\eta')] = \delta_{ij}\delta(\eta - \eta')$. From this point of view, it can be realized that photons in each cavity can leak out to a continuum of states, which is the source of dissipation. We show that this model leads to a Lorentzian spectral density for each dissipative cavity, which implies nonperfect reflectivity of the cavity mirrors. In the following, we assume that each surrounding environment possesses such a narrow bandwidth that only a particular mode of the cavity can be excited [26,33]. This allows one to extend integrals over η back to $-\infty$ and take $G_i(\eta)$ as a constant (equal to $\sqrt{\kappa_i/\pi}$). Then, by introducing the dressed operators $\hat{A}_i(\omega) = \alpha_i(\omega)\hat{a}_i + \int\beta_i(\omega,\eta)\hat{B}_i(\eta)\,d\eta$, one is able to diagonalize Hamiltonian (1), where $\alpha_i(\omega)$ and $\beta_i(\omega,\eta)$ (in general, $\in\mathbb{C}$) are obtained such that $\hat{A}_i(\omega)$ ($i = 1,2$) are annihilation operators obeying the commutation relation $[\hat{A}_i(\omega), \hat{A}_j^\dagger(\omega')] = \delta_{ij}\delta(\omega - \omega')$ [34,35]. The bosonic operator $\hat{a}_i$ can be shown to be a linear combination of the dressed operators $\hat{A}_i(\omega)$ as [26,33]

$$\hat{a}_i = \int \alpha_i^*(\omega)\hat{A}_i(\omega)\,d\omega, \quad (2)$$

with

$$\alpha_i(\omega) = \frac{\sqrt{\kappa_i/\pi}}{\omega - \omega_{c_i} + i\kappa_i}. \quad (3)$$

From this point of view, one can dedicate that, in each cavity the interaction between the qubit and the surrounding environment is governed by terms like $g_i\int(\hat{\sigma}_i^+\alpha_i^*(\omega)\hat{A}_i(\omega) + \mathrm{H.c.})d\omega$. Henceforth, the Hamiltonian describing each atom-cavity dissipative system in the rotating-wave approximation and in units of $\hbar = 1$ can be rewritten in terms of the dressed operators as

$$\hat{H}_{(\mathrm{AF})_i} = \frac{1}{2}\omega_{\mathrm{qb}_i}\hat{\sigma}_{z_i} + \int\omega\hat{A}_i^\dagger(\omega)\hat{A}_i(\omega)\,d\omega + g_i\int[\hat{\sigma}_i^+\alpha_i^*(\omega)\hat{A}_i(\omega) + \mathrm{H.c.}]d\omega, \quad (4)$$

in which ω_{qb_i} and $\hat{\sigma}_{z_i}$ are the atomic transition frequency and population inversion operator of the ith qubit, respectively. The time-dependent Schrödinger equation with Hamiltonian (4) can be solved when the environment initially is in a vacuum state regardless of the state of the qubit. Formally, it is convenient to work in the interaction picture. The Hamiltonian, (4), in the interaction picture, is given by

$$\hat{\mathfrak{V}}_{(\mathrm{AF})_i} = e^{i\hat{H}_{0(\mathrm{AF})_i}t}\hat{H}^{\mathrm{Int}}_{(\mathrm{AF})_i}e^{-i\hat{H}_{0(\mathrm{AF})_i}t}, \quad (5)$$

in which

$$\hat{H}_{0(\mathrm{AF})_i} = \frac{1}{2}\omega_{\mathrm{qb}_i}\hat{\sigma}_{z_i} + \int\omega\hat{A}_i^\dagger(\omega)\hat{A}_i(\omega)\,d\omega,$$
$$\hat{H}^{\mathrm{Int}}_{(\mathrm{AF})_i} = g_i\int[\hat{\sigma}_i^+\alpha_i^*(\omega)\hat{A}_i(\omega) + \mathrm{H.c.}]\,d\omega. \quad (6)$$

After some manipulation, the explicit form of the Hamiltonian in the interaction picture may be obtained as

$$\hat{\mathfrak{V}}_{(\mathrm{AF})_i} = g_i\int[\hat{\sigma}_i^+\alpha_i^*(\omega)e^{i(\omega_{\mathrm{qb}_i}-\omega)t}\hat{A}_i(\omega) + \mathrm{H.c.}]\,d\omega. \quad (7)$$

Without loss of generality, we assume that the two subsystems are similar, i.e., $\omega_{\mathrm{qb}_1} = \omega_{\mathrm{qb}_2} \equiv \omega_{\mathrm{qb}}$, $\omega_{c_1} = \omega_{c_2} \equiv \omega_c$,

$g_1 = g_2 \equiv g$, and $\kappa_1 = \kappa_2 \equiv \kappa$. It should be noted that the analytical solution of the time-dependent Schrödinger equation with an arbitrary initial state seems to be a very hard task, if not impossible. Therefore, we suppose that there is no excitation in the cavities before the occurrence of an interaction and each atom is in the coherent superposition of the exited $|e_i\rangle$ and ground state $|g_i\rangle$ as

$$|\psi_{\mathrm{AF}}(0)\rangle_i = (\cos(\theta_i/2)|e_i\rangle + \sin(\theta_i/2)e^{i\phi_i}|g_i\rangle)|\mathbf{0}\rangle_{R_i}, \quad (8)$$

in which $|\mathbf{0}\rangle_{R_i} = \hat{A}_i(\omega)|1_\omega\rangle_i$ is the multimode vacuum state of the ith environment, where $|1_\omega\rangle_i = \hat{A}_i^\dagger(\omega)|\mathbf{0}\rangle_{R_i}$ is the multimode state of the ith environment representing one photon at frequency ω and the vacuum state in all other modes. In the above relation $\theta_i \in [0,\pi]$ and $\varphi_i \in [0,2\pi]$ for $i = 1,2$. Accordingly, the quantum state of the ith system at any time t can be written as

$$|\psi_{\mathrm{AF}}(t)\rangle_i = C_i(t)|e_i\rangle|\mathbf{0}\rangle_{R_i} + D_i(t)|g_i\rangle|\mathbf{0}\rangle_{R_i} + \int U_{\omega_i}(t)|1_\omega\rangle|g_i\rangle\, d\omega, \quad (9)$$

where $C_i(t)$, $D_i(t)$, and $U_{\omega_i}(t)$ are unknown coefficients that should be determined. Using the time-dependent Schrödinger equation ($i|\dot{\psi}\rangle = \hat{\mathfrak{H}}|\psi\rangle$), one arrives at the set of coupled integrodifferential equations

$$\dot{C}_i(t) = -ig\int \alpha^*(\omega)e^{i\delta_\omega t}U_{\omega_i}(t)\, d\omega, \quad (10a)$$

$$\dot{D}_i(t) = 0, \quad (10b)$$

$$\dot{U}_{\omega_i}(t) = -ig\alpha(\omega)e^{-i\delta_\omega t}C_i(t), \quad (10c)$$

where $\delta_\omega \equiv \omega_{\mathrm{qb}} - \omega$. The second differential equation of the above set can be easily solved as $D_i(t) = D_i(0) = \sin(\theta_i/2)e^{i\phi_i}$. After lengthy but straightforward manipulations, the following integrodifferential equation for the amplitude $C_i(t)$ can be obtained:

$$\dot{C}_i(t) = -\int_0^t f(t-t_1)C_i(t_1)\, \mathrm{d}t_1, \quad (11)$$

where $f(t-t_1)$ is the correlation function relating to the spectral density $J(\omega)$ of the environment as

$$f(t-t_1) = \int d\omega J(\omega)e^{-i\delta_\omega(t-t_1)}, \quad (12)$$

in which, according to Eq. (3), the spectral density reads

$$J(\omega) \equiv g^2|\alpha(\omega)|^2 = \frac{1}{\pi}\frac{g^2\kappa}{(\omega-\omega_c)^2+\kappa^2}. \quad (13)$$

The parameter κ is connected to the damping time of the environment $\tau_B \approx \kappa^{-1}$, which is much longer than its correlation time, over which the correlation functions of the reservoir vanish [36]. On the other hand, it can be shown that the relaxation time τ_R over which the state of the system changes reads $\tau_R \approx g^{-1}$ [37].

A glance at Eq. (13) reveals that the spectral density is a Lorentzian distribution, which implies the nonperfect reflectivity of the cavity mirrors [24]. This leads to an exponentially decaying correlation function, with κ as the decay rate factor of the cavity as follows:

$$f(t-t_1) = g^2e^{-\kappa(t-t_1)}e^{-i\Delta(t-t_1)}, \quad (14)$$

in which $\Delta = \omega_c - \omega_{\mathrm{qb}}$ is the detuning parameter. We note that, by choosing special values of κ, it is possible to extract the ideal cavity and the Markovian limits. The former is obtained when $\kappa \to 0$, which leads to $J(\omega) = g^2\delta(\omega-\omega_0)$, corresponding to a constant correlation function in which $\delta(\cdot)$ is the usual Dirac delta function. In this situation, the system reduces to the usual JCM [38] with the vacuum Rabi frequency $\Omega_R = g$. On the other hand, for small correlation times and by taking κ much larger than any other frequency scale, the Markovian regime may be obtained. For the other generic values of κ, the model interpolates between these two limits.

At any rate, with the help of Laplace transform technique one is able to solve the integrodifferential equation (11), as

$$C_i(t) = C_i(0)\mathcal{E}(t), \quad (15)$$

in which

$$\mathcal{E}(t) \equiv e^{-(i\Delta+\kappa)t/2}\left(\cosh(\Omega t/2) + \frac{i\Delta+\kappa}{\Omega}\sinh(\Omega t/2)\right). \quad (16)$$

Here $\Omega = \sqrt{\kappa^2 - \Omega_R^2 + 2i\Delta\kappa}$, in which $\Omega_R = \sqrt{\Delta^2+4g^2}$. The obtained analytical expression for the amplitude $C_i(t)$ is exact and therefore outside of the Markovian regime. It should be noted that the exact solution presented in (15) for strong- and weak-coupling regimes is due to the Lorentzian spectral density, which has been directly extracted from our modeling of dissipative cavity. For other kinds of spectral densities, only the weak-coupling regime is amenable to a general analysis [39].

III. ENTROPY EVOLUTION OF THE SUBSYSTEMS

In this section, we investigate the dynamical behavior of entanglement between a qubit and its surrounding environment in each subsystem. It is well known that the linear entropy is a promising quantity to measure the amount of entanglement between the qubit and its surrounding environment field, which is defined as [40]

$$S_A(\theta,\phi;t) = 1 - \mathrm{Tr}\left(\hat{\rho}_A^2\right), \quad (17)$$

in which $\hat{\rho}_A$ is the atomic reduced density matrix for each subsystem. The linear entropy can range between 0, corresponding to a completely pure state, and $(1-1/d)$, corresponding to a completely mixed state, in which d is the dimension of the density matrix (here, $d = 2$). Using Eq. (9), the explicit form of the atomic reduced density operator at any time can be derived by tracing over environment variables, which results in

$$\hat{\rho}_A(t) = \begin{pmatrix} |C(t)|^2 & C(t)D^*(t) \\ D(t)C^*(t) & 1-|C(t)|^2 \end{pmatrix}, \quad (18)$$

in which we have dropped the subscript i from coefficients $C_i(t)$ and $D_i(t)$ (and also from parameters θ_i and ϕ_i) because only one subsystem is considered. It is interesting that it is possible to have an input-independent parameter. This can be done by computing the average linear entropy with respect to

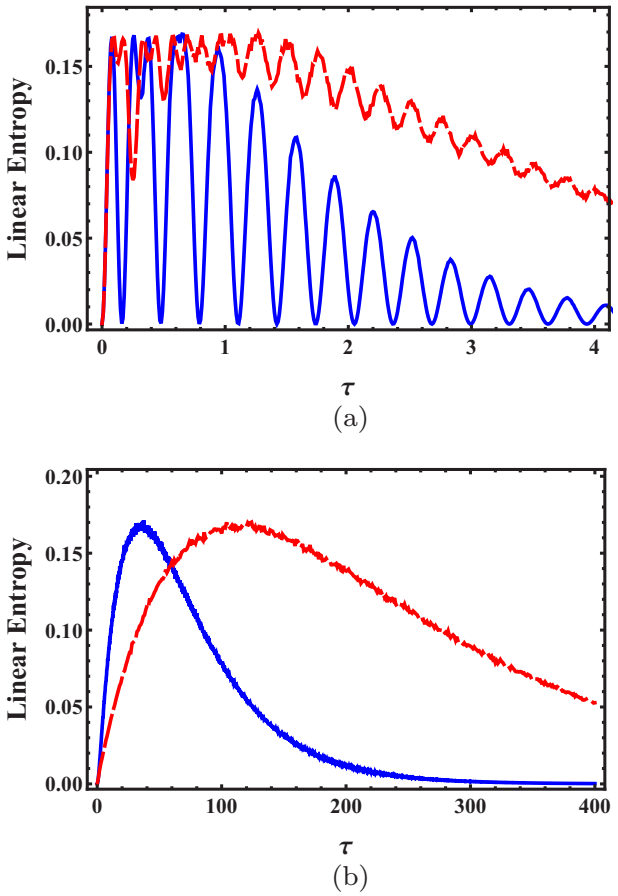

FIG. 2. Time evolution of the average linear entropy as a function of the scaled time τ for (a) the strong-coupling regime, i.e., $R = 10$ with $\Delta = 0$ (solid blue line) and $\Delta = 15\kappa$ (dashed red line), and (b) the weak-coupling regime, i.e., $R = 0.1$ with $\Delta = 0$ (solid blue line) and $\Delta = 1.5\kappa$ (dashed red line).

all possible input states on the surface of the Bloch sphere as

$$S_A^{\rm av}(t) = \int S_A(\theta,\phi;t)\, d\Omega, \tag{19}$$

in which $d\Omega$ is the normalized SU(2) Haar measure. This is related to the concept of entangling power [30].

According to Eqs. (15) and (18), the effective dynamics of the linear entropy depends on the function $\mathcal{E}(t)$. It is noteworthy that from Eq. (16) two distinct weak- and strong-coupling regimes can be distinguished by introducing the dimensionless parameter $R = g/\kappa$, by which we are able to analyze our results in two regimes, good ($R \gg 1$) and bad ($R \ll 1$) cavities. In the bad-cavity limit, the relaxation time is greater than the reservoir correlation time and the variation of the linear entropy is essentially a Markovian exponential behavior. In the good-cavity limit, the reservoir correlation time is greater than the relaxation time and non-Markovian effects such as revival and oscillation of entanglement become dominant. The latter effects are indeed due to the long memory of the environment.

Figure 2 illustrates the average linear entropy as a function of the scaled time $\tau = \kappa t$ for both strong- and weak-coupling regimes in the absence and presence of detuning. In the strong-coupling regime and in the absence of the detuning parameter, the entropy has an oscillatory decaying behavior which represents a non-Markovian process. These revivals and oscillations are due to the memory depth of the reservoir. This can be understood from the fact that, in the strong-coupling regime, the environment feeds back some of the information which it has taken during the interaction with the qubit. In the presence of the detuning parameter, the entanglement sudden death is no longer seen. The linear entropy remains alive at longer intervals of time. On the other hand, in the weak-coupling regime, the linear entropy starts from 0, increases monotonically up to its maximum value, and then drops and decreases until it vanishes. Again, the detuning parameter makes the entropy survive for longer times. Actually, for both coupling regimes and for sufficiently high values of the detuning parameter, it is possible to have a quasistationary entanglement.

IV. ENTANGLEMENT SWAPPING

As observed, there is no direct interaction among the two $(\mathrm{AF})_i$ $(i = 1,2)$ systems, therefore, their states are expected to remain separable,

$$\hat{\rho}(t) = |\Psi(t)\rangle\langle\Psi(t)|, \tag{20}$$

where $|\Psi(t)\rangle = |\psi_{\rm AF}(t)\rangle_1 \otimes |\psi_{\rm AF}(t)\rangle_2$. However, thanks to the results in the previous section, where it is established that the states of the atom-field are entangled in each cavity, in line with the goals of our paper, it is now quite reasonable to search for a strategy to exchange the entanglement between the atom-field in each cavity and the atom-atom (and/or field-field) for the sake of quantum information processing purposes. In this regard, one could think of creating entanglement between the two atoms by performing BSM on the field modes leaving the cavities (see Fig. 1). Mathematically speaking, this can be done by projection $|\Psi(t)\rangle$ onto one of the Bell states of the cavity fields. Among the different types of resources for linear optical quantum swapping implementations, two-photon pairs have been put forward as an efficient resource for our purposes, which are [41]

$$|\Psi^{\pm}\rangle_{\rm F} = \frac{1}{\sqrt{2}}(|\mathbf{0}\rangle_{R_1}|\mathbf{1}\rangle_{R_2} \pm |\mathbf{0}\rangle_{R_1}|\mathbf{1}\rangle_{R_2}), \tag{21a}$$

$$|\Phi^{\pm}\rangle_{\rm F} = \frac{1}{\sqrt{2}}(|\mathbf{0}\rangle_{R_1}|\mathbf{0}\rangle_{R_2} \pm |\mathbf{1}\rangle_{R_1}|\mathbf{1}\rangle_{R_2}), \tag{21b}$$

in which $|\mathbf{0}\rangle_{R_i}$ has been defined before and

$$|\mathbf{1}\rangle_{R_i} \equiv \int \Theta(\omega)|1_\omega\rangle_i\, d\omega, \tag{22}$$

where $\int|\Theta(\omega)|^2 d\omega = 1$, with $\Theta(\omega)$ the pulse shape associated with the incoming photon. Using the introduced Bell-type states, one can easily construct the desired projection operator $P_{\rm F} = |M\rangle_{\rm FF}\langle M|$, in which $M \in \{\Psi^{\pm},\Phi^{\pm}\}$. Consequently, operating the projection operator onto $|\Psi(t)\rangle$ leaves the field states in a Bell-type state and also establishes an entangled atom-atom state. In the next two subsections, we onsider the projection operator based on the Bell states $|\Psi^-\rangle$ and $|\Phi^+\rangle$ and investigate the resulting entanglement properties of the atom-atom states. It should be noted that the other two Bell states can also straightforwardly be taken into account.

A. Bell state $|\Psi^-\rangle_F$

Let us now consider the projection operator

$$P_F^- = |\Psi^-\rangle_{FF}\langle\Psi^-|, \tag{23}$$

whose action on $|\Psi(t)\rangle$ in (20) leaves the field states in the Bell state $|\Psi^-\rangle_F$ and establishes the atom-atom state (after normalization)

$$\begin{aligned}|\Psi_{AA}(t)\rangle &= P_F^-|\Psi(t)\rangle \\ &= \frac{1}{\sqrt{N^-(t)}}\{X_{12}(t)|e,g\rangle - X_{21}(t)|g,e\rangle \\ &\quad + [\Upsilon_{12}(t) - \Upsilon_{21}(t)]|g,g\rangle\},\end{aligned} \tag{24}$$

in which the normalization coefficient reads as

$$N^-(t) = |X_{12}(t)|^2 + |X_{21}(t)|^2 + |\Upsilon_{12}(t) - \Upsilon_{21}(t)|^2. \tag{25}$$

Here, we have defined

$$X_{jk}(t) = C_j(t)\int \mathbf{d}\omega\Theta^*(\omega)U_{\omega_k}(t)e^{-i\omega t}, \tag{26a}$$

$$\Upsilon_{jk}(t) = D_j(t)\int \mathbf{d}\omega\Theta^*(\omega)U_{\omega_k}(t)e^{-i\omega t}. \tag{26b}$$

In order to quantify the amount of entanglement between the two atoms, we use the concurrence, which has been defined as [29]

$$E(\hat{\rho}(t)) = \max\{0,\sqrt{\lambda_1} - \sqrt{\lambda_2} - \sqrt{\lambda_3} - \sqrt{\lambda_4}\}, \tag{27}$$

where $\lambda_i, i = 1,2,3,4$ are the eigenvalues (in decreasing order) of the Hermitian matrix $\hat{\rho}_{AA}(\sigma_1^y \otimes \sigma_2^y \hat{\rho}_{AA}^* \sigma_1^y \otimes \sigma_2^y)$, with $\hat{\rho}_{AA}^*$ the complex conjugate of $\hat{\rho}_{AA}$ and $\sigma_k^y := i(\sigma_k - \sigma_k^\dagger)$. The concurrence varies between 0 (completely separable) and 1 (maximally entangled). For the state, (24), concurrence reads as

$$E(\hat{\rho}(t)) = \frac{T_1(t,\theta_1,\theta_2)}{T_1(t,\theta_1,\theta_2) + T_2(\theta_1,\theta_2,\phi_1,\phi_2)}, \tag{28}$$

in which

$$T_1(t,\theta_1,\theta_2) = 2\cos^2(\theta_1/2)\cos^2(\theta_2/2)|\mathcal{E}(t)|^2, \tag{29a}$$

$$\begin{aligned}T_2(\theta_1,\theta_2,\phi_1,\phi_2) &= \frac{1}{2}[1 - \cos\theta_1\cos\theta_2 \\ &\quad - \sin\theta_1\sin\theta_2\cos(\phi_1 - \phi_2)].\end{aligned} \tag{29b}$$

The surprising aspect here is that the resulting concurrence does not depend on the pulse shape of the incoming photon [i.e., $\Theta(\omega)$]. Before considering the time evolution of the resulting concurrence, it is interesting that, for certain conditions, state (24) can have a unique stationary state. A glance at (28) reveals that whenever $T_2(\theta_1,\theta_2,\phi_1,\phi_2) = 0$, the concurrence would be independent of time and it always remains at its maximum value, i.e., 1. According to Eq. (29b), this condition is fulfilled with the set of solutions

$$\theta_1 = \theta_2 \quad \text{and} \quad \phi_1 - \phi_2 = 2m\pi, \quad m = 0, \pm 1, \tag{30}$$

which leads to the maximally entangled Bell state (up to an irrelevant global phase)

$$|\Psi^-\rangle = \frac{1}{\sqrt{2}}(|e,g\rangle - |g,e\rangle). \tag{31}$$

Quite generally, the concurrence, (28), depends on the initial state. However, it is logical to state that our model is a good entangler when the average of the final swapped entanglement over all possible initial states is positive. This statistical average over the initial states establishes an input-independent dynamics of entanglement. Therefore, we use the concept of entangling power, which is defined as [30]

$$\mathfrak{E}(t) := \int E(\rho(t))\, d\mu(|\psi(0)\rangle), \tag{32}$$

where $d\mu(|\psi(0)\rangle)$ is the probability measure over the submanifold of product states in $\mathbb{C}^2 \otimes \mathbb{C}^2$. The latter is induced by the Haar measure of SU(2) $\otimes$ SU(2). Specifically, referring to the parametrization of (8), it reads

$$d\mu(|\psi(0)\rangle) = \frac{1}{16\pi^2}\prod_{k=1}^{2}\sin\theta_k \mathrm{d}\theta_k d\varphi_k. \tag{33}$$

This measure is normalized to 1. It is trivial that in this case the entangling power $\mathfrak{E}$ lies in [0,1].

As stated before, two distinct regimes, strong and weak coupling, can be distinguished. Figure 3 illustrates the entangling

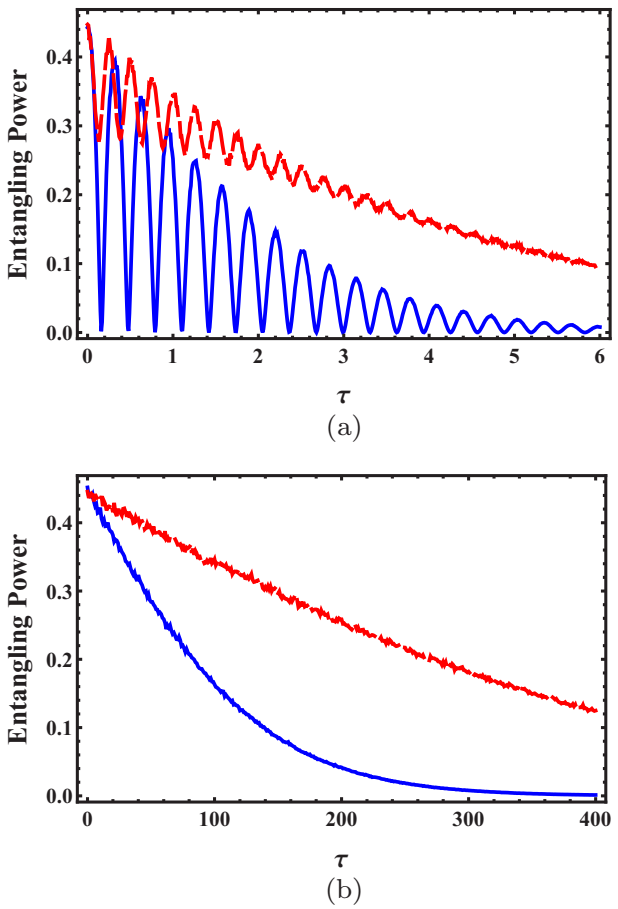

FIG. 3. Time evolution of the entangling power of the atom-atom state after BSM ($P_F^- = |\Psi^-\rangle_{FF}\langle\Psi^-|$) as a function of the scaled time τ for (a) the strong-coupling regime, i.e., $R = 10$ with $\Delta = 0$ (solid blue line) and $\Delta = 15\kappa$ (dashed red line), and (b) the weak-coupling regime, i.e., $R = 0.1$ with $\Delta = 0$ (solid blue line) and $\Delta = 1.5\kappa$ (dashed red line).

power as a function of the scaled time $\tau = \kappa t$ in the absence and presence of detuning for both coupling regimes. In the strong-coupling regime, an oscillatory behavior of entanglement is seen due to the long memory effect of the cavities. In both cases the entangling power has a decaying behavior in the absence and presence of the detuning parameter. The detuning parameter has a crucial role in surviving the swapped entanglement. Especially, in the strong-coupling regime, it completely suppresses the entanglement's sudden death.

B. Bell state $|\Phi^+\rangle_F$

Let us now consider another Bell state, i.e., $|\Phi^+\rangle_F$, in order to construct the projection operator $P_F^+ = |\Phi^+\rangle_{FF}\langle\Phi^+|$. It is straightforward to obtain the following (normalized) atom-atom state by applying this new projection operator to state (20):

$$\begin{aligned}|\Psi_{AA}(t)\rangle &= P_F^+|\Psi(t)\rangle \\ &= \frac{1}{\sqrt{N^+}}\{C_1(t)C_2(t)|e,e\rangle + C_1(t)D_2(t)|e,g\rangle \\ &\quad + D_1(t)C_2(t)|g,e\rangle \\ &\quad + [D_1(t)D_2(t) + C_1(0)C_2(0)\Gamma(t)^2]|g,g\rangle\}, \quad (34)\end{aligned}$$

in which

$$\Gamma(t) = -ig\int_0^t dt_1\mathcal{E}(t_1)e^{i\omega_{qb}(t-t_1)}\int d\omega\alpha(\omega)\Theta^*(\omega)e^{-i\omega(t-t_1)}. \quad (35)$$

In the above relations, the normalization coefficient is

$$\begin{aligned}N^+ &\equiv N^+(t,\theta_1,\theta_2,\phi_1,\phi_2) \\ &= \cos^2(\theta_1/2)\cos^2(\theta_2/2)[|\mathcal{E}(t)|^4 + |\Gamma(t)|^4] \\ &\quad + 0.5|\mathcal{E}(t)|^2(1-\cos\theta_1\cos\theta_2) + \sin^2(\theta_1/2)\sin^2(\theta_2/2) \\ &\quad - 0.5\sin\theta_1\sin\theta_2\mathrm{Re}[e^{-i(\phi_1+\phi_2)}\Gamma^2(t)]. \quad (36)\end{aligned}$$

For state (34) the concurrence explicitly reads as

$$E(\hat{\rho}(t)) = \frac{T(t,\theta_1,\theta_2)}{N^+(t,\theta_1,\theta_2,\phi_1,\phi_2)}, \quad (37)$$

in which

$$T(t,\theta_1,\theta_2) = 2\cos^2(\theta_1/2)\cos^2(\theta_2/2)|\mathcal{E}(t)|^2|\Gamma(t)|^2. \quad (38)$$

Unlike the previous case, the concurrence depends on the pulse shape of the incoming photon, i.e., $\Theta(\omega)$. Therefore, different pulse shapes lead to different behaviors of the dynamics of entanglement. However, due to the technical difficulties arising when calculating the integrals, (35), we consider the incoming pulse shape to be exactly the same as (3). With this assumption, the function $\Gamma(t)$ explicitly becomes

$$\Gamma(t) = -2ie^{-(i\Delta+\kappa)t/2}\frac{g}{\Omega}\sinh(\Omega t/2). \quad (39)$$

Quite generally, the concurrence, (37), is 0 at any time for $\theta_1 = \theta_2 = \pi$. This condition corresponds to initial atomic state $|g,g\rangle$ (up to a global phase). Here, no entanglement can be created because no excitation can be exchanged between the two qubits by the action of BSM. Moreover, according to (34) and (36) the final state after BSM is $|g,g\rangle$ (up to an irrelevant global phase), which clearly is a separable state.

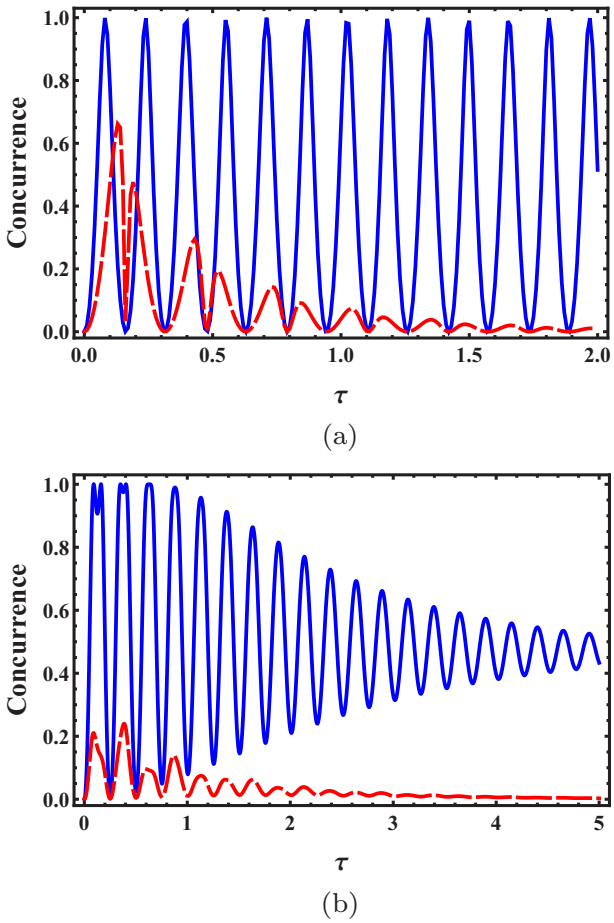

FIG. 4. Time evolution of the concurrence of the atom-atom state after BSM ($P_F^+ = |\Phi^+\rangle_{FF}\langle\Phi^+|$) as a function of the scaled time τ for the strong-coupling regime, i.e., $R = 10$ for (a) $\Delta = 0$ and (b) $\Delta = 15\kappa$, with $\theta_1 = \theta_2 = 0$ (solid blue line) and $\theta_1 = \theta_2 = \pi/2$ and $\phi_1 = \phi_2 = 0$ (dashed red line).

On the other hand, we expect that the concurrence reaches its maximum value for $\theta_1 = \theta_2 = 0$. This corresponds to the initial atomic state $|e,e\rangle$. It is straightforward to show that with these values, the concurrence is maximum whenever the following condition is fulfilled:

$$|\mathcal{E}(t)| = |\Gamma(t)|. \quad (40)$$

However, due to the presence of parameter g in the expression of $\Gamma(t)$, this condition can only be fulfilled in the strong-coupling regime. In order to see this phenomenon explicitly, let us plot the concurrence for some initial states in both coupling regimes.

In Fig. 4 we have plotted the time evolution of the concurrence, (37), as a function of the scaled time $\tau = \kappa t$ in the strong-coupling regime (i.e., $R = 10$) for two initial atomic states in the absence and presence of the detuning parameter. Let us first investigate the case in which the exact resonance condition is considered. As shown in Fig. 4(a) (solid curve), for initial atomic state $|e,e\rangle$ (i.e., $\theta_1 = \theta_2 = 0$) and in the absence of the detuning parameter ($\Delta = 0$), the concurrence has an oscillatory behavior between 0 and its maximum value (i.e., 1). Therefore, despite the presence of dissipation, it is possible to

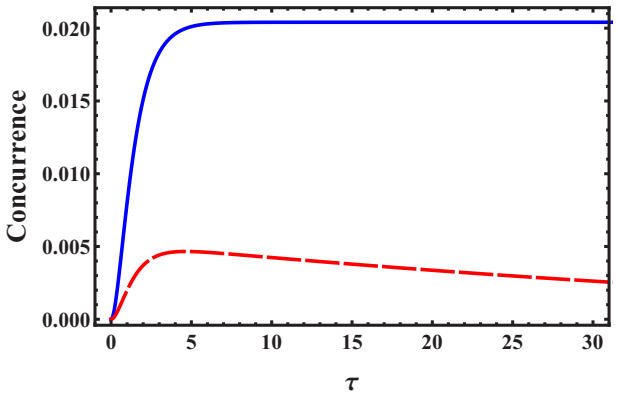

FIG. 5. Time evolution of the concurrence of the atom-atom state after BSM ($P_{\mathrm{F}}^{+} = |\Phi^{+}\rangle_{\mathrm{FF}}\langle\Phi^{+}|$) as a function of the scaled time τ for the weak-coupling regime, i.e., $R = 0.1$ in the absence of the detuning parameter (i.e., $\Delta = 0$) for $\theta_1 = \theta_2 = 0$ (solid blue line) and $\theta_1 = \theta_2 = \pi/2$ and $\phi_1 = \phi_2 = 0$ (dashed red line).

achieve the maximum amount of entanglement. The maximum value of entanglement is obtained whenever condition (40) is fulfilled, which straightforwardly takes us to the following scaled times τ_n at which the concurrence is maximum:

$$\tau_n = \frac{1}{10}\left(2n\pi + \frac{\pi}{4}\right), \tag{41}$$

where n is an integer. At these times, it is straightforward to show that, $\mathcal{E}(t)$ and $\Gamma(t)$ become real functions of time, and consequently the atom-atom state is projected into the following Bell state:

$$|\Psi_{\mathrm{AA}}\rangle = \frac{1}{\sqrt{2}}(|e,e\rangle + |g,g\rangle). \tag{42}$$

For another atomic initial state (i.e., $\theta_1 = \theta_2 = \pi/2$) and in the absence of the detuning parameter, an oscillatory and decaying behavior of concurrence is seen [see Fig. 4(a); dashed curve]. The entanglement sudden death phenomenon is clearly seen and no stationary entanglement is created.

In the presence of the detuning parameter and for $\theta_1 = \theta_2 = 0$, the oscillatory and decaying behavior of the concurrence is clearly seen. However, the entanglement's sudden death is no longer observed. As the scaled time goes on, the amplitude of oscillations decreases until the concurrence reaches the stationary value (here it is about 0.47). Our further calculations (not shown here) illustrate that, as the detuning parameter increases, the stationary value of concurrence decreases. For other initial states, the detuning parameter causes concurrence to vanish in shorter scaled times.

Figure 5 illustrates the resulting concurrence as a function of the scaled time τ in the weak-coupling regime for zero detuning parameter with different initial atomic states. The weak-coupling regime shows different behavior. In this regime and for $\theta_1 = \theta_2 = 0$, the concurrence starts at 0, increases monotonically up to the stationary value, and then remains fixed at this value as time goes on. The amount of swapped entanglement is negligible in comparison to that in the strong-coupling regime. This can be explained by paying attention to the fact that in the weak-coupling regime, the correlation between a typical qubit and its environment is too weak.

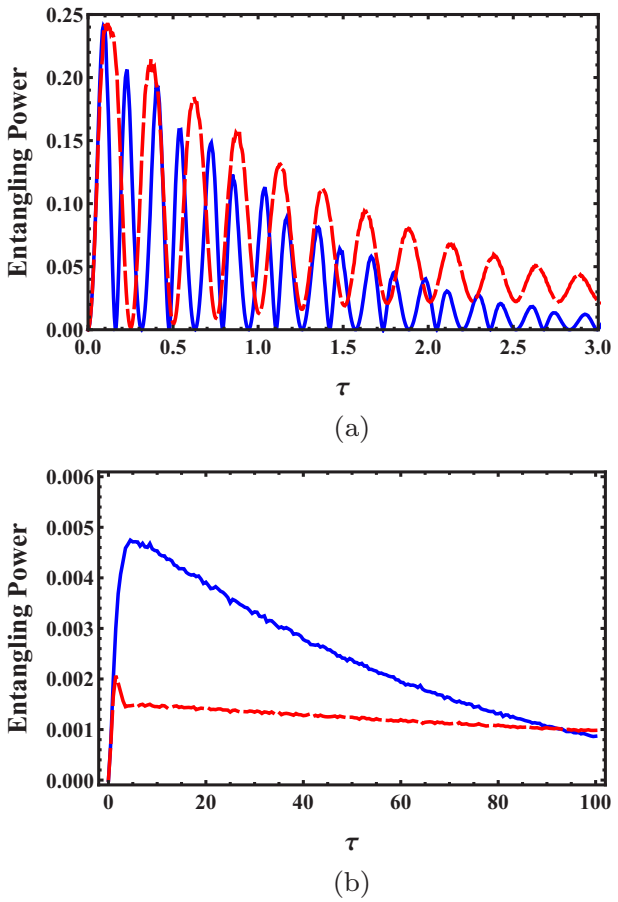

FIG. 6. Time evolution of the entangling power of the atom-atom state after BSM as a function of the scaled time τ for (a) the strong-coupling regime, i.e., $R = 10$ with $\Delta = 0$ (solid blue line) and $\Delta = 15\kappa$ (dashed red line) and (b) the weak-coupling regime, i.e., $R = 0.1$ with $\Delta = 0$ (solid blue line) and $\Delta = 1.5\kappa$ (dashed red line).

Therefore, the amount of swapped entanglement must be less than that in the strong-coupling regime. As explained before, the concurrence never reaches its maximum value in this regime. For another initial state, the stationary concurrence no longer exists. Finally, it should be noted that our further calculations show that the presence of the detuning parameter decreases considerably the amount of stationary concurrence.

Having ascribed the role of the initial state in the dynamics of swapped entanglement, we examine, on average, how much entanglement can be swapped between the two qubits. For this purpose, we have plotted the entangling power as a function of the scaled time $\tau = \kappa t$ for the two strong- and weak-coupling regimes in the absence and presence of the detuning parameter (see Fig. 6). In the strong-coupling regime, oscillatory behavior of the entangling power with a decaying envelope is clearly observed. In the absence of the detuning parameter the entanglement sudden death phenomenon is clearly seen.

In the weak-coupling regime, on average, the amount of entanglement is negligible in comparison with that in the strong-coupling regime. However, a small amount of entanglement is seen in the presence of the detuning parameter.

V. CONCLUDING REMARKS

To sum up, we have considered two independent dissipative cavities, each consisting of a qubit. In each dissipative cavity, the qubit interacts with a single-mode field and the field interacts with a set of continuum harmonic oscillators. Therefore, the leakage of photons into a continuum of states is the source of dissipation. This allows us to investigate our results outside of the Markovian limit. However, by introducing a set of dressed operators $\hat{A}_i(\omega)$ which contain the information of the cavity field and the surrounding environment, we have solved the time-dependent Schrödinger equation and obtained the analytical expression of the state vector of each subsystem for special initial conditions.

Then, before considering the entanglement swapping protocol, we have investigated the dynamics of entanglement between each qubit and its surrounding environment. This has been done by evaluating the average of the linear entropy measure over all possible initial states of the qubit. The results show that oscillatory decaying behavior of the entropy is seen in the strong-coupling regime and in the absence of the detuning parameter. These oscillations are due to the long memory of the environment. However, this behavior does not occur in the weak-coupling regime, where the behavior of the entropy is monotonically decaying. In the presence of the detuning parameter, the linear entropy survives for longer intervals of time in both regimes.

Next, we have implemented the entanglement swapping protocol to transform entanglement from two atom-field subsystems to atom-atom by an interference measurement performed on fields leaving the cavities (BSM). This has been done by projecting the state of the entire system onto one of the Bell states of the cavity fields. We have presented our results for two types of field-field Bell-type states. First, we consider the $|\Psi^-\rangle_{\rm F}$ Bell state. In this case, the resulting concurrence does not depend on the pulse shape of incoming photons. Furthermore, for $\theta_1 = \theta_2$ and $\phi_1 - \phi_2 = 2m\pi$ $(m = 0, \pm 1)$, the atom-atom state has the unique stationary state $|\Psi^-\rangle = \frac{1}{\sqrt{2}}(|e,g\rangle - |g,e\rangle)$. In order to investigate the dynamical behavior of swapped entanglement, we introduced the entangling power, (32). Again, oscillatory behavior of the entanglement is seen for the strong-coupling regime. In both regimes, the swapped entanglement shows decaying behavior. However, the detuning parameter plays a crucial role in surviving the swapped entanglement.

On the other hand, for the field-field Bell state $|\Phi^+\rangle_{\rm F}$, the situation differs slightly. First, the resulting concurrence depends directly on the pulse shape of incoming photons. By assuming that the pulse shape is the same as $\alpha(\omega)$, it is possible to solve the relevant integrals and obtain the analytical expression for the concurrence. Second, unlike the previous case, there is not a unique entangled stationary state, but for $\theta_1 = \theta_2 = \pi$ the concurrence is 0 at any time t. In the strong-coupling regime, for initial atomic state $|e,e\rangle$ (i.e., $\theta_1 = \theta_2 = 0$), and in the absence of the detuning parameter ($\Delta = 0$), oscillatory (without decaying) behavior of the concurrence is seen. Our results show that at discrete (scaled) times $\tau_n = \frac{1}{10}(2n\pi + \frac{\pi}{4})$, where n is an integer, the concurrence reaches its maximum value and the atom-atom state is projected into the maximally entangled Bell state $\frac{1}{\sqrt{2}}(|e,e\rangle + |g,g\rangle)$. Furthermore, the amount of swapped entanglement in the weak-coupling regime is negligible in comparison with that in the strong-coupling regime.

Finally, we should emphasize that our results can be helpful in designing implementations for entanglement swapping when environmental effects cannot be neglected. For instance, recently, it has been proven that a hyperentanglement swapping protocol which is based on the hyperentanglement Bell state measurement can discriminate 16 Bell states in both polarization and spatial mode degrees of freedom [42]. It is also shown that it is possible to perform long-distance quantum communication based on the logic-qubit entanglement when environmental effects are not considered [43]. Based on our presented formalism, our idea can be extended to an arbitrary number of qubits in their own dissipative environments [27]. Therefore, our results could be useful for discriminating an arbitrary number of Bell states based on the hyperentanglement and logic-qubit entanglement swapping when they suffer from noise. Furthermore, our proposal has the potential ability to consider a number of qubits in each dissipative cavity. In this way, the qubits inside each dissipative cavity can be considered a Bose-Einstein condensate in an optical cavity [44] in the presence of thermal noise. Then the output of the optical cavity of each node is sent to an intermediate site where a Bell-like detection is performed on these optical pairs [44]. Finally, recalling the crucial role of entanglement swapping in the development of real devices for the application of quantum information theory, such as the development of quantum computers and quantum remote state preparation, whenever the subsystems unavoidably interact with their environment, our proposal can be expected to be a first step towards such protocols.

[1] R. Horodecki, P. Horodecki, M. Horodecki, and K. Horodecki, Rev. Mod. Phys. **81**, 865 (2009).

[2] A. K. Ekert, Phys. Rev. Lett. **67**, 661 (1991).

[3] S. L. Braunstein and A. Mann, Phys. Rev. A **51**, R1727 (1995).

[4] K. Mattle, H. Weinfurter, P. G. Kwiat, and A. Zeilinger, Phys. Rev. Lett. **76**, 4656 (1996).

[5] T. Richter and W. Vogel, Phys. Rev. A **76**, 053835 (2007).

[6] M. Murao, D. Jonathan, M. B. Plenio, and V. Vedral, Phys. Rev. A **59**, 156 (1999).

[7] Q. A. Turchette, C. S. Wood, B. E. King, C. J. Myatt, D. Leibfried, W. M. Itano, C. Monroe, and D. J. Wineland, Phys. Rev. Lett. **81**, 3631 (1998).

[8] B. Julsgaard, A. Kozhekin, and E. S. Polzik, Nature (London) **413**, 400 (2001).

[9] A. Aspect, P. Grangier, and G. Roger, Phys. Rev. Lett. **47**, 460 (1981).

[10] A. Izmalkov, M. Grajcar, E. Il'ichev, T. Wagner, H.-G. Meyer, A. Y. Smirnov, M. H. S. Amin, A. Maassen van den Brink, and A. M. Zagoskin, Phys. Rev. Lett. **93**, 037003 (2004).

[11] H. R. Baghshahi, M. K. Tavassoly, and M. J. Faghihi, Laser Phys. **24**, 125203 (2014).
[12] E. T. Jaynes and F. W. Cummings, Proc. IEEE **51**, 89 (1963).
[13] M. Żukowski, A. Zeilinger, M. A. Horne, and A. K. Ekert, Phys. Rev. Lett. **71**, 4287 (1993).
[14] S. Bose, V. Vedral, and P. L. Knight, Phys. Rev. A **57**, 822 (1998).
[15] R. E. S. Polkinghorne and T. C. Ralph, Phys. Rev. Lett. **83**, 2095 (1999).
[16] X. Jia, X. Su, Q. Pan, J. Gao, C. Xie, and K. Peng, Phys. Rev. Lett. **93**, 250503 (2004).
[17] B.-S. Shi, Y.-K. Jiang, and G.-C. Guo, Phys. Rev. A **62**, 054301 (2000).
[18] Q. H. Liao, G. Y. Fang, Y. Y. Wang, M. A. Ahmad, and S. Liu, Eur. Phys. J. D **61**, 475 (2011).
[19] M. Ghasemi and M. K. Tavassoly, Eur. Phys. J. Plus, in press (2016).
[20] N. Lee, H. Benichi, Y. Takeno, S. Takeda, J. Webb, E. Huntington, and A. Furusawa, Science **332**, 330 (2011).
[21] R. Daneshmand and K. M. Tavassoly, Eur. Phys. J. D **70**, 1 (2016).
[22] F.-G. Deng, X.-H. Li, C.-Y. Li, P. Zhou, and H.-Y. Zhou, Eur. Phys. J. D **39**, 459 (2006).
[23] M. Rafiee, A. Nourmandipour, and S. Mancini, Phys. Rev. A **94**, 012310 (2016).
[24] H.-P. Breuer and F. Petruccione, *The Theory of Open Quantum Systems* (Oxford University Press, New York, 2002).
[25] A. Nourmandipour and M. K. Tavassoly, Eur. Phys. J. Plus **130**, 1 (2015).
[26] A. Nourmandipour and M. K. Tavassoly, J. Phys. B: At. Mol. Opt. Phys. **48**, 165502 (2015).
[27] A. Nourmandipour, M. K. Tavassoly, and M. Rafiee, Phys. Rev. A **93**, 022327 (2016).
[28] A. Nourmandipour, M. K. Tavassoly, and M. A. Bolorizadeh, J. Opt. Soc. Am. B **33**, 1723 (2016).
[29] W. K. Wootters, Phys. Rev. Lett. **80**, 2245 (1998).
[30] P. Zanardi, C. Zalka, and L. Faoro, Phys. Rev. A **62**, 030301 (2000).
[31] M.-Y. Ye, D. Sun, Y.-S. Zhang, and G.-C. Guo, Phys. Rev. A **70**, 022326 (2004).
[32] R. F. Abreu and R. O. Vallejos, Phys. Rev. A **73**, 052327 (2006).
[33] S. M. Dutra, *Cavity Quantum Electrodynamics: The Strange Theory of Light in a Box* (John Wiley & Sons, New York, 2005).
[34] U. Fano, Phys. Rev. **124**, 1866 (1961).
[35] S. M. Barnett and P. M. Radmore, *Methods in Theoretical Quantum Optics*, Vol. 15 (Oxford University Press, New York, 2002).
[36] C. Gardiner and P. Zoller, *Quantum Noise: A Handbook of Markovian and Non-Markovian Quantum Stochastic Methods with Applications to Quantum Optics*, Vol. 56 (Springer Science & Business Media, New York, 2004).
[37] B. Bellomo, R. Lo Franco, and G. Compagno, Phys. Rev. Lett. **99**, 160502 (2007).
[38] M. Tavis and F. W. Cummings, Phys. Rev. **170**, 379 (1968).
[39] A. Kofman and G. Kurizki, Nature (London) **405**, 546 (2000).
[40] N. A. Peters, T.-C. Wei, and P. G. Kwiat, Phys. Rev. A **70**, 052309 (2004).
[41] S.-W. Lee and H. Jeong, *Proceedings of the First International Conference on Entangled Coherent State and Its Application to Quantum Information Science* (Tamagawa University, Tokyo, 2012), pp. 41–46.
[42] Y.-B. Sheng, F.-G. Deng, and G. L. Long, Phys. Rev. A **82**, 032318 (2010).
[43] L. Zhou and Y.-B. Sheng, Phys. Rev. A **92**, 042314 (2015).
[44] M. Eghbali-Arani, H. Yavari, M. A. Shahzamanian, V. Giovannetti, and S. Barzanjeh, J. Opt. Soc. Am. B **32**, 798 (2015).